J Mater Sci (2013) 48:7603–7612
DOI 10.1007/s10853-013-7577-1

FEM simulation of the hygro-thermal behaviour of wood under surface densification at high temperature

Stefania Fortino · Andrea Genoese · Alessandra Genoese · Lauri Rautkari

Received: 6 February 2013 / Accepted: 4 July 2013 / Published online: 24 July 2013

Abstract Surface densification of solid wood increases the density on the surface, when compressed by single side heated press. A recent experimental study has pointed out the influence of the process parameters on the development of the density profiles in the modified samples. Numerical modelling can help to optimize the experimental work which is often time consuming and laborious due to the large amount of experiments required to check the influence of the pressing parameters. In the present work, a FEM simulation of the hygro-thermal behaviour of wood under surface densification is proposed by using a three-dimensional hygro-thermal model based on earlier literature approaches. The model is implemented in a user subroutine of the FEM code Abaqus starting from the definition of a weak form of the governing hygro-thermal equations of the problem. The numerical profiles of moisture content and temperature during the wood densification process are simulated for some wood specimens tested in a previous study. Conclusions are given on the relationship between these profiles and the experimental density profiles due to different process parameters.

S. Fortino (✉)
VTT Technical Research Centre of Finland, P.O. Box 1000, 02044 Espoo, Finland
e-mail: stefania.fortino@vtt.fi

A. Genoese · A. Genoese
Department of Engineering Modelling, University of Calabria, Via P. Bucci, Cubo 39/b, 87036 Arcavacata di Rende, CS, Italy
e-mail: andreagenoese_83@hotmail.it

A. Genoese
e-mail: alessandrag_83@hotmail.it

L. Rautkari
School of Chemical Technology, Aalto University, P.O. Box 16400, 00076 Aalto, Espoo, Finland
e-mail: lauri.rautkari@aalto.fi

L. Rautkari
Forest Products Research Institute, Joint Research Institute for Civil and Environmental Engineering, School of Engineering and the Built Environment, Edinburgh Napier University, 10 Colinton Road, Edinburgh EH10 5DT, UK

Introduction

Solid wood can be compressed in radial direction under certain conditions, when wood material is softened above its glass transition temperature (T_g) which is highly dependent on its moisture content [1–3]. Rather than compressing solid wood throughout, the densification can be targeted on the surface only [4–6]. Therefore, the process can be short, only few minutes, and less energy is needed for the modification. The surface densification process has several phases. First, a relatively dry wood specimen is heated only on one surface in contact with a hot plate and compressed by an unheated plate during a process phase called *closing time*. After the unheated loading plate has contacted with the stops of the device, the press remains closed and the heating continues during the *holding time* phase. Furthermore, a cooling system is turned on during the phase of *cooling time*, while the load is maintained until the temperature is below a fixed value. It is well known that wood panel boards (e.g. particle board) suffer immediately spring back after pressing, if the press is opened when wood material is in soften state. Cooling phase decreases the immediately spring back after the press is opened. However, some spring back still occurs [7, 8] because of the stored internal stresses. An important feature of the process is that the compression in radial direction does not produce major fractures [4] of the cell walls above the glass transition point. The surface densification affects both the

hygro-thermal behaviour of wood and its mechanical properties. The result of this process can be an environmental friendly product, since no toxic chemicals needed and only heat and moisture, showing several potentialities in different sectors of the wood industry [9].

In the last few years, the experimental research on wood surface densification has pointed out the influence of various process parameters (wood species, initial moisture content, press temperature, closing time, holding time and compression ratio) on the development of density profiles in the treated samples [4, 5]. This knowledge is very useful to obtain optimal properties for the treated wood. Due to the large amount of experiments required to check the influence of the process parameters for wood surface densification, the experimental approach may be rather time consuming and laborious. For this reason, numerical modelling can significantly help to optimize the experimental work. To numerically simulate the full process of wood surface densification, an accurate hygro-thermal model is required for the description of simultaneous transport of heat and moisture inside the wood. In the existing literature, several numerical models for the hygro-thermal behaviour of wood-based composites under hot-pressing processes are available [10–14]. In addition, a large amount of scientific papers are available on the numerical modelling of drying and high-temperature treatment of solid wood as, among others [15–20]. These earlier models provide precious suggestions for the hygro-thermal modelling of surface densification in solid wood.

The importance of temperature and moisture content levels coupled with heat and mass transfer in wood is pointed out in an earlier study [21]. In the same study, the use of computational modelling for a realistic prediction of the quantities inside the wood is strongly suggested. Multi-physics is a primary tool to be used for solving the coupled problems occurring in wood at high temperatures, and the exploitation of material properties assessed by micromechanics and multiscale modelling can improve the understanding of these phenomena in future [22].

In the present work, a three-dimensional FEM model for simulation of hygro-thermal phenomena characterizing wood surface densification is used which is a specialization of the multiphase model previously proposed in [17] by adding the modelling of convection used in [11, 12] and [14–16]. Employed mathematical model is based on the conservation equations for energy, air and moisture content, taking into account both the hygroscopic (or bound) water and the water vapour phase, while the free water is neglected as moisture contents remain below the fibre saturation point. Flow of bound water through the solid occurs only by molecular diffusion while air and steam transport includes both diffusion and convection. System of three coupled PDEs describing the process is solved through the commercial FEM code Abaqus [23], where a special finite element is programmed into the user subroutine Uel [24].

The presented model is used to numerically simulate the distribution of moisture content and temperature in wood samples tested under surface densification within a previous study [4]. The correspondence between the available peaks of density measured during the experiments and the numerical peaks of moisture content and temperature is discussed. The proposed computational approach is particularly suitable as the first step for a 3D full hygro-thermo-mechanical FEM simulation of wood surface densification also when other mechanical loads are applied.

A variant of previous multiphase models for wood at high temperatures

The wood densification process involves the simultaneous transfer of heat and mass. Thus, it is necessary to analyse moisture, air and heat transport throughout the material. The existing literature on this topic has been re-visited and a model has been selected which is a specialization of the one at proposed in [17] for high-temperature treatment of wood. This model has been slightly modified and then integrated with the approaches presented in [11, 12] and [14–16] for the modelling of convection. In the following, the matrix and vector forms of the tensors involved in the partial differential equations governing the problem will be used.

In this work, the following assumptions were done:

1. The values of bound water diffusion and thermal conduction parameters in radial and tangential directions are assumed to be equal. Since wood exhibits a larger anisotropy between the cross sectional plane and the longitudinal direction (compared to the anisotropy in the cross sectional plane), different diffusion parameters are used in the longitudinal direction [25]. However, the material parameters for diffusive and convective fluxes for vapour and air are assumed to be the same in all directions [17].
2. The earlywood and latewood rings are not considered as different materials [25].
3. Since the positions of wood piths were located very far from the cut samples in order to have the growth ring as parallel as possible, a rectangular coordinate system (with tangential, radial and longitudinal directions along the X-Y-Z axis) is used in the numerical simulations.
4. At each point of the material, local equilibrium between bound water and vapour water is assumed, with a sorption isotherm that couples the moisture contents in the solid and the vapour phase.
5. Ideal gas behaviour is considered for the gaseous phases.

According to an earlier study [17], the mass balance equations for water and dry air are described by Eqs. 1 and 2, respectively:

$$\frac{\partial \varrho_b}{\partial t} + \varepsilon \frac{\partial \varrho_v}{\partial t} + \nabla \cdot (\mathbf{J}_b + \mathbf{J}_v) = 0 \tag{1}$$

$$\varepsilon \frac{\partial \varrho_a}{\partial t} + \nabla \cdot \mathbf{J}_a = 0 \tag{2}$$

where $\mathbf{J}_b$, $\mathbf{J}_v$ and $\mathbf{J}_a$ represent the flux vectors of the bound water (b), water vapour (v), and air (a) respectively, ϱ_b is the bound water concentration with the dry wood (d) volume as reference, ϱ_v and ϱ_a are the concentrations of the gaseous phases referred to the lumens volume, so porosity $\varepsilon = 1 - \varrho_d/1500$ is the volume of voids with respect to the one of dry wood whose density is ϱ_d. Finally t is the time, ∇ collects the derivatives with respect to the coordinates x, y and z in space and $(\cdot)$ indicates the dot product.

Let M be the moisture content per unit mass of dry wood, Eq. 1 becomes:

$$\varrho_d \frac{\partial M}{\partial t} + \nabla \cdot (\mathbf{J}_b + \mathbf{J}_v) = 0 \tag{3}$$

By exploiting Fick's law, the flux of bound water becomes $\mathbf{J}_b = -\varrho_d \mathbf{D}_b \nabla M_b$ where $M_b = \varrho_b/\varrho_d = M - \varepsilon \varrho_v/\varrho_d$ and $\mathbf{D}_b$ represents the diffusion matrix of bound water. The diffusion coefficient in the radial and tangential directions is calculated as in [17] and its value is multiplied by an amplification factor of 2.5 when referring to the longitudinal direction.

As pointed out in [11] and [12], during high-temperature processes and in particular in hot-pressing cases, the diffusion of air and steam is a minor phenomenon compared to convection. According to [11], if the velocity of the gaseous mixture is expressed by means of the Darcy law, the diffusive and convective fluxes for vapour and air are defined as

$$\mathbf{J}_v^d = -\frac{m_v}{RT}\mathbf{D}_{\text{eff}} \nabla P_v, \quad \mathbf{J}_v^c = -\frac{m_v}{RT\eta_g}\mathbf{K}_g P_v \nabla P_g \tag{4}$$

$$\mathbf{J}_a^d = -\frac{m_a}{RT}\mathbf{D}_{eff} \nabla P_a, \quad \mathbf{J}_a^c = -\frac{m_a}{RT\eta_g}\mathbf{K}_g P_a \nabla P_g \tag{5}$$

where $\mathbf{D}_{\text{eff}}$ represents the effective diffusivity matrix and $\mathbf{K}_g = k_g \mathbf{I}$ the relative permeability matrix for the gas flow, $\mathbf{I}$ being the identity matrix and k_g a relative permeability coefficient. $\mathbf{D}_{\text{eff}} = \boldsymbol{\delta} D_{va}$ is obtained from the so-called inter-diffusion coefficient of an air–vapour mixture D_{va} used in [16] where $\boldsymbol{\delta} = \delta \boldsymbol{I}$ is a reduction matrix accounting for the porous structure and the tortuous path of wood, δ being the attenuation factor.

Furthermore, in Eqs. (4) and (5) m_a and P_a, m_v and P_v represent the molar mass and the partial pressure for the dry air and the vapour, respectively; R and T are the ideal gas constants and the temperature; $P_g = P_v + P_a$ and η_g represent the total pressure and the dynamic viscosity of the air–vapour mixture, respectively. Viscosity η_g is taken from [26], while the partial vapour pressure P_v is related to the so-called saturation partial pressure of water vapour P_{sv} by means of the following sorption isotherm used in [17] as a function of moisture content and temperature:

$$P_v = P_{sv}(T)\psi(M,T) \tag{6}$$

where $P_{sv} = \exp\left(25.5058 - \frac{5204.9}{T}\right)$ and

$$\psi = \exp\left[\left(17.884 - 0.1423T + 23.63 \times 10^{-5}T^2\right) \times \left(1.0237 - 67.4 \times 10^{-5}T\right)^{92M}\right]$$

The temperature dependence of the sorption isotherm in wood is an important phenomenon in particular in the presence of high temperatures (see [27–29] for more details).

To complete the formulation of the problem, the conservation of energy is expressed in the form used in [17]:

$$\varrho c_p \frac{\partial T}{\partial t} = \nabla \cdot (\mathbf{K}\nabla T + h_b \mathbf{J}_b + h_v \mathbf{J}_v + h_a \mathbf{J}_a) \tag{7}$$

where $\mathbf{K}$ is the thermal conductivity matrix, $\varrho c_p = \varrho_d(c_{pd} + M_b c_{pw}) + \varepsilon \varrho c_{pg}$ is the total heat capacity, c_{pd} and c_{pw} being the specific heats of the dry wood and water and $\varrho c_{pg} = \varrho_v c_{pv} + \varrho_a c_{pa}$ refers to the gas mixture depending of the specific heats c_{pa} and c_{pv} of the two gas phases. Finally h_b, h_v, h_a are the specific enthalpies of air, steam and bound water. The thermal conductivity $\mathbf{K}$ is calculated by the classical approach described in [30], starting from the value in the transversal direction. For the longitudinal direction amplification by 2.5 is considered. Standard expressions for the enthalpies of bound water and the different gaseous phases are taken from [16, 17]. Finally for the specific heats, the values proposed in [31] are used for steam and air, while the expressions reported in [17] are adopted for dry wood and water.

Introducing also the hypothesis of ideal gas behaviour for air and steam, after some manipulations, Eqs. (2) and (3) can be rewritten as

$$\varepsilon \frac{\partial \varrho_a}{\partial t} = \nabla \cdot (\mathbf{D}_{AA}\nabla \varrho_a + \mathbf{D}_{AM}\nabla M + \mathbf{D}_{AT}\nabla T) \tag{8}$$

$$\varrho_d \frac{\partial M}{\partial t} = \nabla \cdot (\mathbf{D}_{MA}\nabla \varrho_a + \mathbf{D}_{MM}\nabla M + \mathbf{D}_{MT}\nabla T) \tag{9}$$

where the various matrices are:

$$\mathbf{D}_{AA} = \frac{P_a}{\eta_g}\mathbf{K}_g + \mathbf{D}_{\text{eff}}, \qquad \mathbf{D}_{AM} = \frac{m_a}{RT}\frac{P_a}{\eta_g}P_{sv}\frac{\partial \psi}{\partial M}\mathbf{K}_g,$$

$$\mathbf{D}_{MA} = \frac{m_v P_v}{m_a \eta_g}\mathbf{I},$$

$$\mathbf{D}_{AT} = \frac{m_a}{RT}\frac{P_a}{\eta_g}\mathbf{K}_g\left(\varrho_a \frac{R}{m_a} + \frac{\partial P_{sv}}{\partial T}\psi + \frac{\partial \psi}{\partial T}P_{sv}\right) + \frac{\varrho_a}{T}\mathbf{D}_{\text{eff}},$$

$$\mathbf{D}_{MMv} = \frac{m_v}{RT}\left(\frac{P_v}{\eta_g}\mathbf{K}_g + \mathbf{D}_{\text{eff}}\right)P_{sv}\frac{\partial\psi}{\partial M},$$
$$\mathbf{D}_{MMb} = \varrho_d\left(1 - \frac{\varepsilon}{\varrho_d}\frac{m_v}{RT}P_{sv}\frac{\partial\psi}{\partial M}\right)\mathbf{D}_b, \quad (10)$$
$$\mathbf{D}_{MTb} = \frac{\varepsilon m_v}{RT}\left\{\frac{P_v}{T} - \left(\frac{\partial P_{sv}}{\partial T}\psi + \frac{\partial\psi}{\partial T}P_{sv}\right)\right\}\mathbf{D}_b,$$
$$\mathbf{D}_{MTv} = \frac{m_v}{RT}\left\{\frac{P_v}{\eta_g}\mathbf{K}_g\frac{\varrho_a R}{m_a} + \left(\frac{P_v}{\eta_g}\mathbf{K}_g + \mathbf{D}_{eff}\right)\left(\frac{\partial P_{sv}}{\partial T}\psi + \frac{\partial\psi}{\partial T}P_{sv}\right)\right\},$$
$$\mathbf{D}_{MM} = \mathbf{D}_{MMv} + \mathbf{D}_{MMb}, \quad \mathbf{D}_{MT} = \mathbf{D}_{MTv} + \mathbf{D}_{MTb}$$

By using the same notation, the energy balance is

$$\varrho c_p\frac{\partial T}{\partial t} = \nabla\cdot(\mathbf{D}_{TA}\nabla\varrho_a + \mathbf{D}_{TM}\nabla M + \mathbf{D}_{TT}\nabla T) \quad (11)$$

with the matrices $\mathbf{D}_{TA} = h_a\mathbf{D}_{AA} + h_v\mathbf{D}_{MA}$, $\mathbf{D}_{TM} = h_a\mathbf{D}_{AM} + h_v\mathbf{D}_{MMv} + h_b\mathbf{D}_{MMb}$, $\mathbf{D}_{TT} = \mathbf{K} + h_a\mathbf{D}_{AT} + h_v\mathbf{D}_{MTv} + h_b\mathbf{D}_{MTb}$.

The direct consequence of Eq. 6 is that sorption phenomena (see [32] and [28] for a systematic description) are not considered. To include the simulation of sorption, a reformulation of the model and further computational work are needed.

Boundary conditions

Since the hot plate is assumed to be impervious to gas, no gas fluxes are imposed, while a thermal resistance for the contact is assumed as in [12] and [14] that imply the following condition

$$-\mathbf{K}\nabla T\cdot\mathbf{n} = h_{Tp}(T - T_{\text{plate}}) \quad (12)$$

where h_{Tp} represents the heat transfer coefficient at the contact between the wood sample and the hot plate and $\mathbf{n}$ is the outside normal to the surface.

According to [14], the following boundary conditions are imposed for the faces in contact with the ambient air:

$$-(\mathbf{D}_{AA}\nabla\varrho_a + \mathbf{D}_{AM}\nabla M + \mathbf{D}_{AT}\nabla T)\cdot\mathbf{n} = h_p\frac{\varrho_a}{\eta_g}(P_g - P_{\text{amb}}) \quad (13)$$

$$-(\mathbf{D}_{MA}\nabla\varrho_a + \mathbf{D}_{MM}\nabla M + \mathbf{D}_{MT}\nabla T)\cdot\mathbf{n} = h_p\frac{\varrho_v}{\eta_g}(P_g - P_{\text{amb}}) \quad (14)$$

$$-\mathbf{K}\nabla T\cdot\mathbf{n} = h_T(T - T_{\text{amb}}) \quad (15)$$

where the subscript 'amb' refers to the quantities related to the ambient.

The values used for the different material parameters described above are summarized in Table 1.

FEM implementation in Abaqus code

In order to use the model in the FEM commercial code Abaqus, a standard eight-node isoparametric brick element with the same interpolation for all the unknown variables is implemented in the user subroutine Uel [24]. A weak form of the problem presented in the previous section is obtained multiplying Eqs. (8), (9) and (11) by the three weight functions w_A, w_M and w_T and then integrating over the volume V. Introducing a linearization of the functions at the time t starting from the corresponding values at the time $t + \Delta t$ and by applying the product rule and the divergence theorem, the following equations are obtained:

$$\frac{1}{\Delta t}\int_V w_A\varepsilon\left(\varrho_{a,t+\Delta t} - \varrho_{a,t}\right) + \int_V \nabla w_A\cdot(\mathbf{D}_{AA}\nabla\varrho_a + \mathbf{D}_{AM}\nabla M + \mathbf{D}_{AT}\nabla T) - \int_S w_A\mathbf{n}\cdot(\mathbf{D}_{AA}\nabla\varrho_a + \mathbf{D}_{AM}\nabla M + \mathbf{D}_{AT}\nabla T) = 0, \quad \forall w_A$$

Table 1 Material parameters for the wood surface densification modelling

Parameter	Value	Units	Equation	Reference
Heat transfer coefficient at the contact between wood sample and hot plate h_{Tp}	50.0	$\text{Wm}^{-2}\text{K}^{-1}$	12	–
Heat transfer coefficient for lateral surface h_T	20.0	$\text{Wm}^{-2}\text{K}^{-1}$	15	[15]
Edges convection coefficient for pressure h_p	1.0×10^{-11}	m	13–14	[14]
Ambient pressure P_{amb}	101325.0	Pa	13–14	[24]
Ambient temperature T_{amb}	293.15	K	15	–
Relative permeability k_g	5.0×10^{-14}	m^2	4–5	[16]
Molar weight of dry air	0.018015	kg mol^{-1}	4–5	[24]
Molar weight of vapour	0.028964	kg mol^{-1}	4–5	[24]

$$\frac{1}{\Delta t}\int_V w_M \varrho_d \left(M_{,t+\Delta t} - M_{,t}\right) + \int_V \nabla w_M \cdot \left(\mathbf{D}_{MA}\nabla \varrho_a + \mathbf{D}_{MM}\nabla M + \mathbf{D}_{MT}\nabla T\right) - \int_S w_M \mathbf{n}\cdot\left(\mathbf{D}_{MA}\nabla \varrho_a + \mathbf{D}_{MM}\nabla M + \mathbf{D}_{MT}\nabla T\right) = 0, \quad \forall w_M \tag{16}$$

$$\frac{1}{\Delta t}\int_V w_T \varrho c_p \left(T_{,t+\Delta t} - T_{,t}\right) + \int_V \nabla w_T \cdot \left(\mathbf{D}_{TA}\nabla \varrho_a + \mathbf{D}_{TM}\nabla M + \mathbf{D}_{TT}\nabla T\right) - \int_S w_T \mathbf{n}\cdot\left(\mathbf{D}_{TA}\nabla \varrho_a + \mathbf{D}_{TM}\nabla M + \mathbf{D}_{TT}\nabla T\right) = 0, \quad \forall w_T$$

in which the differentiations are equally distributed between the unknowns and the test functions w. Finally, S indicates the boundary surface.

Experimental tests

In this paper, some of the tests presented in [4] are simulated. The tested wood material was the clear sapwood with regular growth rings of kiln dried Scots pine (*Pinus sylvestris* L.) from Southern Finland. An initial moisture content $MC_0 = 9.6$ % was reached in the specimens after 2 months conditioning in relative humidity of 35 %. The initial value for density was $\varrho_d = 530$ kg/m^3 (RH 65 %, 20 °C). More details are given in [4]. The dimensions of the specimens numerically analysed in the present work are 140 mm (longitudinal), 50 mm (tangential) and 16 mm (radial).

The surface densification was obtained by using an electrically heated plate incorporated into a press tool fitted to a Zwick 1475 testing machine combined with an MTS Premium Elite controller (see Fig. 1). The used device included a water cooling system to enable the heated surface of the press tool to be cooled from the maximum reached temperature to below 100 °C within ~30 s. The plate temperature was monitored by a PT-100 sensor below the stainless steel surface. Mechanical stops forced the specimens to be compressed to a target final thickness (15 mm), when compression ratio of 6 % was reached. Earlier studies have been shown that the material properties can be enhanced rather much even with 1-mm compression, especially hardness [5, 6]. Density profiles were measured at intervals of 0.1 mm through the thickness,

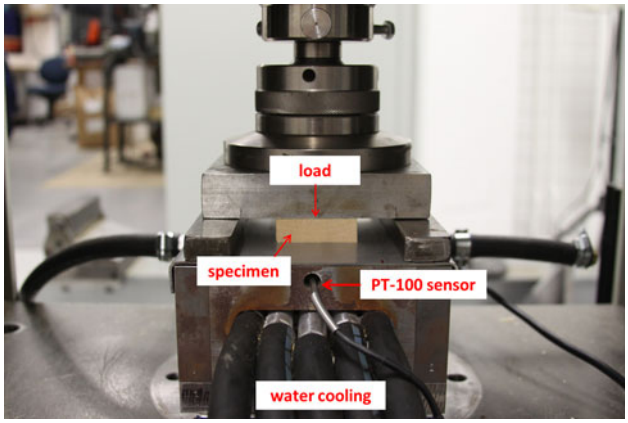

Fig. 1 Device for wood surface densification

using an ATR Density Profilometer DPM201 (1995) using a gamma ray. More details are available in [4]. Some of the results from [4] in terms of density profiles of vertical path of the specimen are reported in the next section.

Numerical results and discussion

In the following, the hygro-thermal responses of the specimens with dimensions, initial conditions and loading rate described in the previous section are simulated under different process parameters. The studied tests are simulated following some assumptions:

- The hygro-thermal analysis is conducted on the undeformed mesh, so the mechanical effects due to the compression rate during closing time are not taken into account. The reason of this choice is that the proposed analysis has to be considered as a first hygro-thermal step to be used within a sequential hygro-thermo-mechanical analysis.
- The dry wood density during the simulation is assumed to be constant and equal to the initial density ($\varrho_d = 530$ kg/m^3).

For all the considered cases, the initial air density is calculated following [25] starting from the vapour pressure value in equilibrium with MC_0 at the temperature $T_0 = 20$ °C, according to the sorption isotherm exploited in this work.

Case a: influence of the holding time

The experiments presented in [4] for a value of initial moisture $MC_0 = 9.6$ %, *heating temperature* $T = 150$ °C, *closing time* = 0.5 min, two different values of *holding*

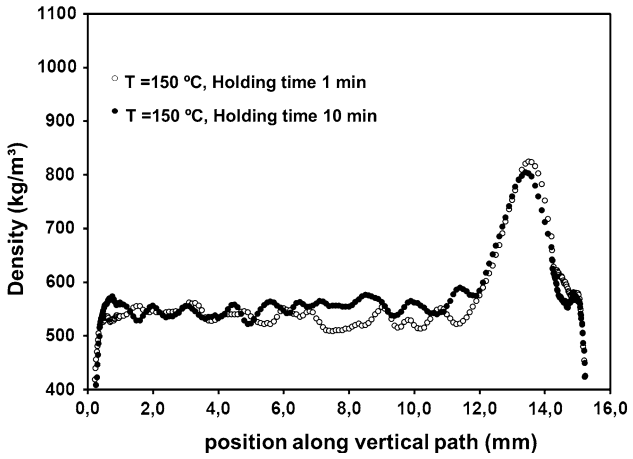

Fig. 2 Case a: influence of the *holding time*. Experimental results. Density profiles along the vertical path at the end of the experimental process

time (1 min and 10 min) and *cooling time* = 0.5 min, were simulated. The test with *holding time* 1 min is taken as reference test for the other cases studied in this work.

The experimental results do not show relevant differences between the reached profiles of density (see Fig. 2). A slightly higher peak of density closer to the hot surface occurs for the case with *holding time* = 1 min, while the density peak is lower and slightly shifted further away from the surface for the case with *holding time* = 10 min. These results can be explained by analysing the numerical profiles of temperature and moisture content (Fig. 4) along the vertical path drawn in Fig. 3 and by the curves of T and MC during time (Fig. 5):

- *End of holding time* For the test with *holding time* 10 min, the higher temperature reached at the end of

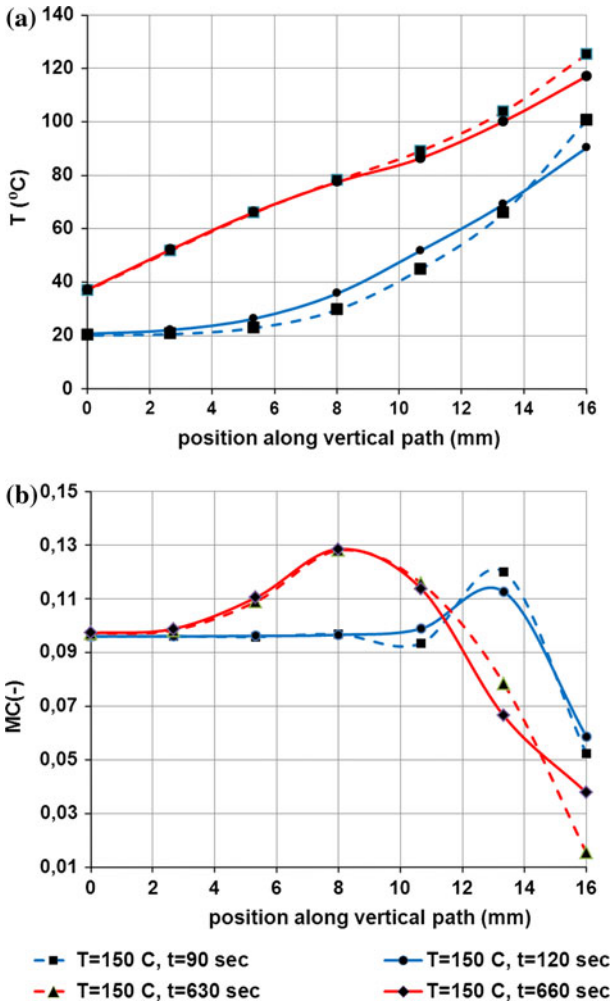

Fig. 4 Case a: influence of the *holding time*. Numerical values of temperature and moisture content along the vertical path of Fig. 3 at the end of *holding time* (t = 90 s and t = 630 s) and at the end of *cooling time* (t = 120 s and t = 660 s). *Top*: T profiles. *Bottom*: MC profiles

Fig. 3 Case a: influence of the *holding time*. Numerical results for the case with *holding time* 1 min. Distribution of moisture content on the undeformed mesh at t = 120 s (end of *cooling time*) and vertical path in the middle of the specimen used for the calculation of temperature and MC profiles (arrow from the surface in contact with the press to the heated surface)

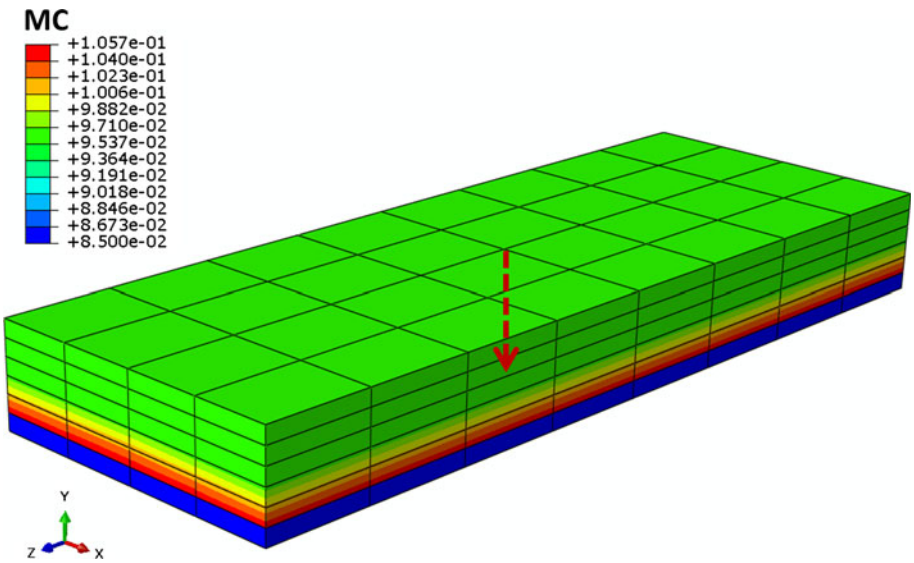

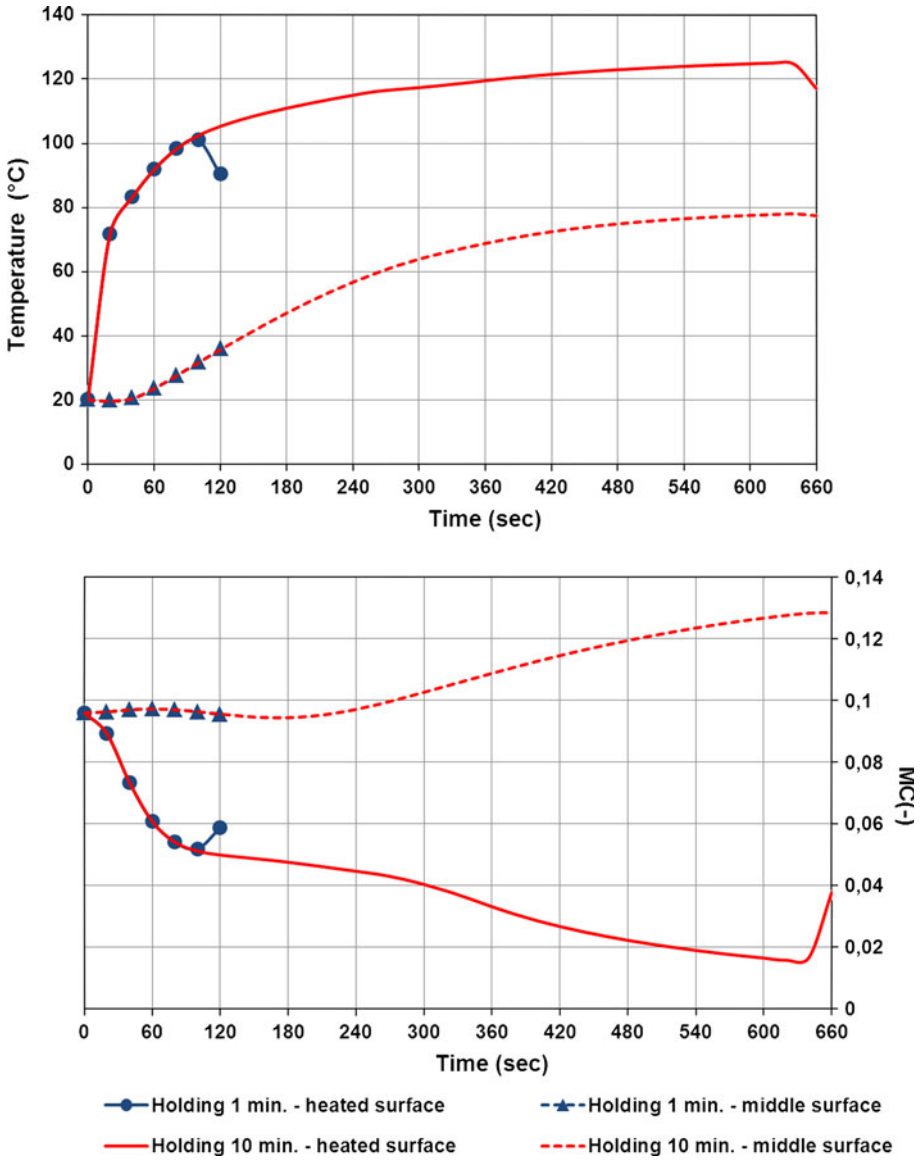

Fig. 5 Case a: influence of the *holding time*. Numerical curves of temperature and moisture content during time on the heated and middle surface of the specimen until the end of *cooling time* ($t = 660$ s). *Top*: T curves. *Bottom*: MC curves

the *holding time* makes the wood surface drier compared to the case with *holding time* 1 min and this causes a bigger reduction of the moisture content on the surface as well as a higher peak of MC shifted away from the surface itself (Fig. 4). On the contrary, the peak of moisture content for the case with *holding time* = 1 min occurs close to the heated surface. This behaviour is explained by the plots of T and MC (Fig. 5). As described in [13] for hot-pressed wood composites, also in the present case the sudden increase of temperature on the surface in contact with the hot press at the end of the *closing time* (30 s) produces a sudden decrease of MC. The gradient of vapour pressure drives the vapour from the surface into the specimen where MC increases. The increase of moisture content on the internal surfaces continues until the end of holding time with a higher growing rate for the case with *holding time* 10 min. This phenomenon produces the shift of the MC peaks towards the middle of the specimen. At the end of *holding time*, the peak of MC for the case with *holding time* 1 min occurs almost in correspondence of the final peak of density while for the case with *holding time* 10 min, the peak of MC appears shifted into the specimen rather far from the position of the final peak of density.

- *End of cooling time* During the *cooling time* there is a slight increase of MC on the external surface and a slight decrease on the internal surface with lower peaks of MC that are located almost in the same positions as the density peaks reached at the end of the densification process.

The above results point out that the response in terms of MC during *holding time* 1 min has a significant influence

on the final position of the density peak. On the other hand, the specimen was compressed only 1 mm. In the case of *holding time* 10 min, the higher peak of MC far from the surface and very close to the middle of the specimen suggests that, in the presence of a larger compression, the final density peak can be more shifted inside the specimen and closer to the reached peak of MC.

Case b: influence of the heating temperature

The test presented in [4] for the case of *closing time* = 0.5 min, *holding time* = 1 min and *cooling time* = 0.5 min with heating temperature $T = 200$ °C was simulated and compared with the numerical results of the reference test (Case a, *closing time* = 0.5 min, *holding time* 1 min, *cooling time* = 0.5 min, $T = 150$ °C).

The experimental profiles of density obtained in [4] show a clear and higher peak of density close to the surface for the case with $T = 150$ °C, while the density peak is lower and slightly shifted further away from the surface for the case with $T = 200$ °C (see Fig. 6). This behaviour is explained in Fig. 7 by the numerical profiles of temperature and moisture content on the vertical path of Fig. 3:

- *End of holding time* In the case with $T = 200$ °C, the high temperature reached at the end of the *holding time* (Fig. 7, top) makes the wood surface drier compared to the case with $T = 150$ °C and a higher peak of MC occurs. In both the compared cases, the peaks of MC are slightly shifted from the external surface into the specimen and remain close to the heated surface. The plots of T and MC during time (Fig. 8) explain the reason of this behaviour, in fact the moisture content on the middle surface shows a low-rate increase until about 1 min from the beginning of the test and then a low-rate decrease.
- *End of cooling time* In both the compared cases, there is a shifting of the MC peaks deeper into the specimen (Fig. 7), but the values of the peaks are reduced due to the decrease of temperature (and increase of moisture content) on the surface (Fig. 8).

The obtained results confirm that the peaks of MC reached at the end of a short *holding time* influence the final position of the peaks of density. The effect of higher temperatures produces a shift of the MC peak from the heated surface which is also in agreement with the shift of density peak obtained from the experiments (Fig. 6). This MC shift is less relevant than the one obtained in Case (a) for *holding time* 10 min and $T = 150$ °C but larger than the shift for *holding time* 1 min and $T = 150$ °C. This result also suggests that, in the presence of a larger compression (more than 1 mm), the

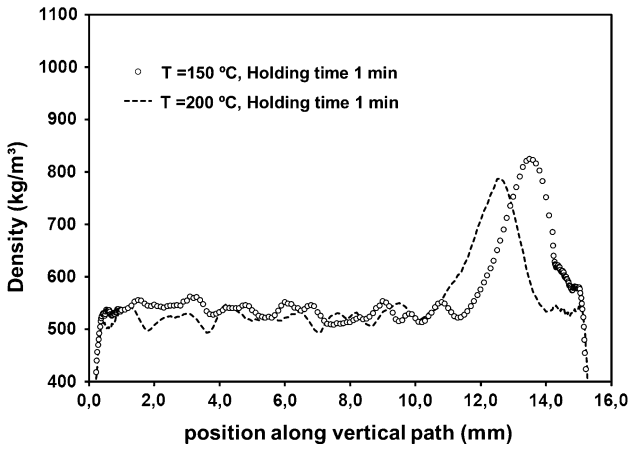

Fig. 6 Case b: influence of the heating temperature. Experimental results. Density profiles along the vertical path at the end of the experimental process

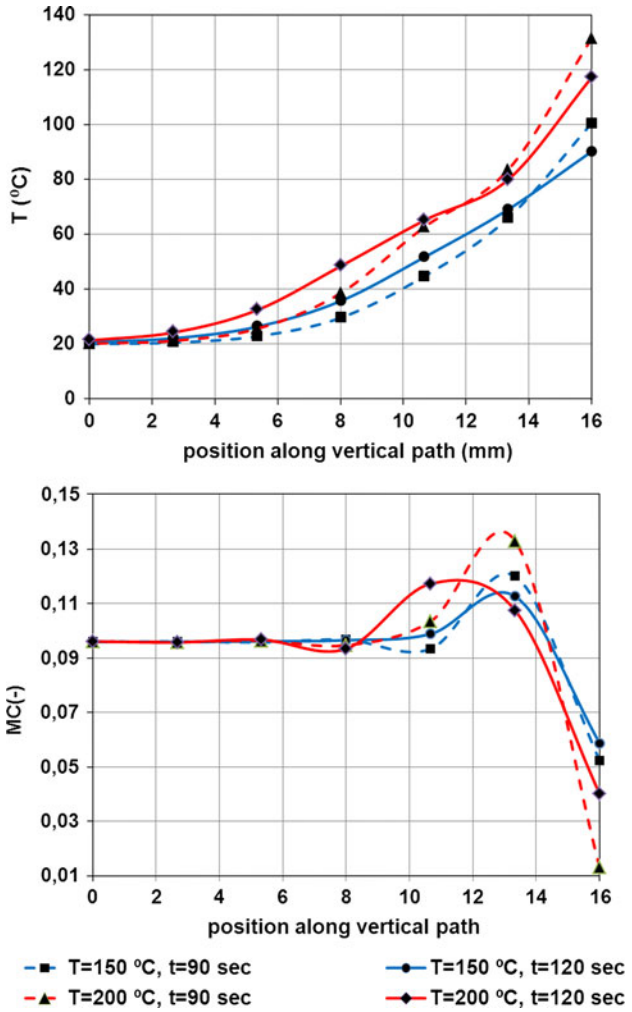

Fig. 7 Case b: influence of the heating temperature. Numerical values of temperature and moisture content along the vertical path of Fig. 3 at the end of *holding time* ($t = 90$ s) and at the end of *cooling time* ($t = 120$ s). *Top*: T profiles. *Bottom*: MC profiles

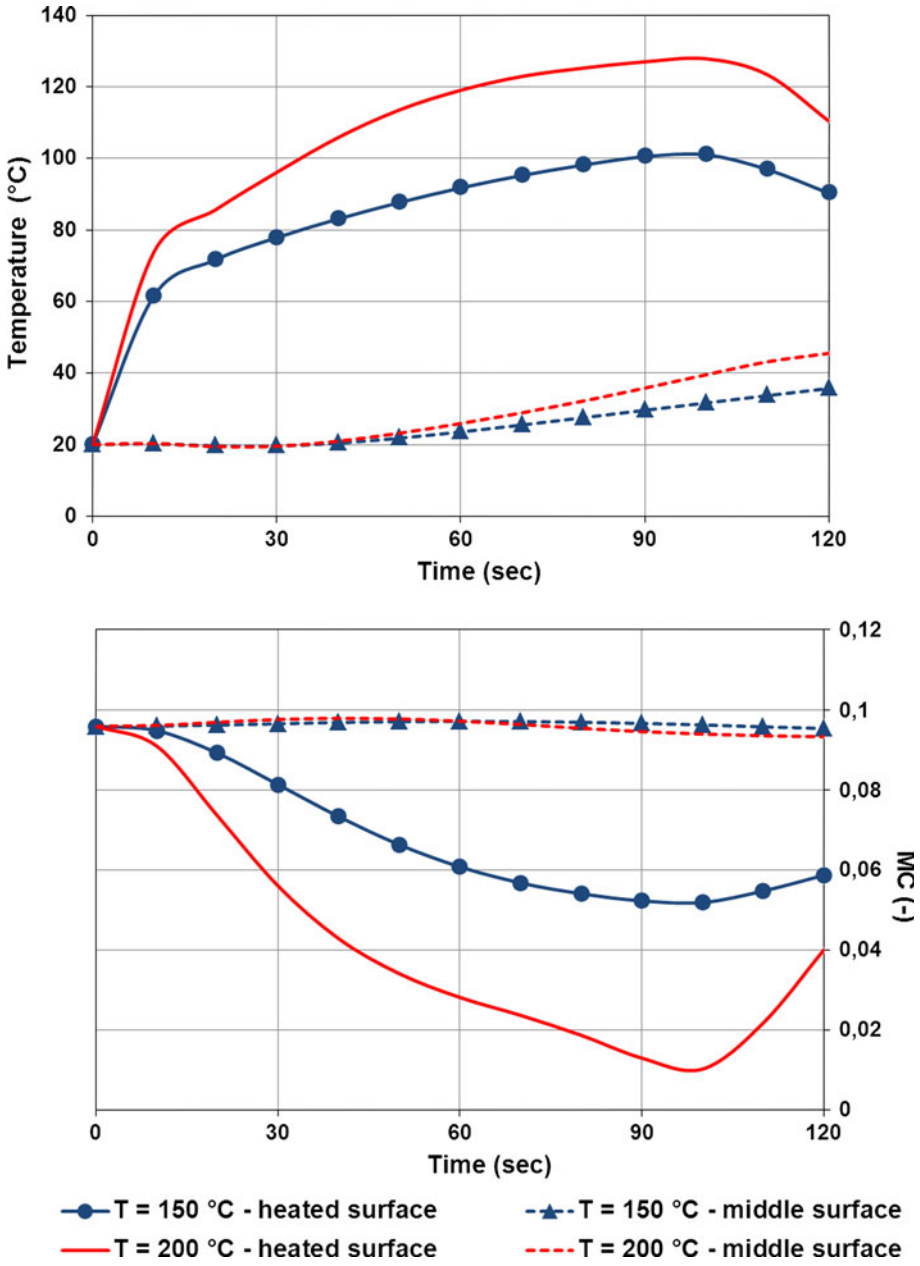

Fig. 8 Case b: influence of the heating temperature. Numerical curves of temperature and moisture content during time on the heated and middle surface of the specimen until the end of *cooling time* ($t = 120$ s). *Top*: T curves. *Bottom*: MC curves

final density peak for $T = 200$ °C and *holding time* $= 1$ min can be closer to the reached MC.

Some notes on future extension of the model

The future extension of the model for a full hygro-thermo-mechanical simulation of the surface densification process in solid wood requires a study of the coupling between hygro-thermal phenomena and mechanical response. For the hot-press cases, in [10] a three-dimensional heat and mass transfer model was combined with a one-dimensional rheological model. Further features can be exploited by referring to other mechanical approaches used for treatment at high temperatures or modelling of wood under compression. Orthotropic-viscoelastic-mechanosorptive models for wood with mechanical variables depending on hygro-thermal quantities were developed mainly for drying cases, for example in [33]. Interesting results on the nonlinear mechanical behaviour of wood under compression can be found in [34] where a material point method (MPM) was used. Special Abaqus user subroutines for inelastic behaviour of wood under compression are developed in [35].

The model proposed in the present paper can be further developed in Abaqus FEM code by transferring the

hygro-thermal results to a mechanical analysis that includes a suitable model for wood under temperature up to 200 °C. A full model can be able to evaluate the reached density and to deeply understand the phenomenon of spring back. This further step is under development.

Conclusion and future work

In this study, the hygro-thermal behaviour of wood during wood surface densification is simulated by using a numerical approach. In this way, it is possible to numerically evaluate the distribution of moisture and temperature inside the material during the treatment, taking into account the phases of bound water and water vapour as well as the dry air involved in the process.

The FEM strategy used to solve the governing equations of the problem is implemented in the Uel subroutine of Abaqus FEM code. The numerical profiles of temperature and moisture content explain the reasons of the differences between the experimental density profiles obtained within a previous study with different values of *holding time* and heating temperature. The presented model does not reproduce experimental results but it gives indications about the near-correspondence of density peaks and the numerical peaks of moisture content and temperature. Further experimental work is needed to verify the model. The experimental measurement for temperature is rather straightforward, but dynamic moisture content measurement will be extremely challenging. The presented method can be considered as a first hygro-thermal step for a full hygro-thermo-mechanical analysis of wood under surface densification.

Acknowledgements This research was supported by the VTT project IMAGO. The Doctorate School of Science and Technique Bernardino Telesio (Doctorate Degree Programme in Computational Mechanics) and the International Mobility funding of University of Calabria, Italy, that allowed the authors Alessandra Genoese and Andrea Genoese to undertake a research stage at VTT, are gratefully acknowledged.

References

1. Salmén L, Kolseth P, Rigdahl M (1986) In: Salmén L, de Ruvo A, Seferis JC, Stark EB (eds.) Composite systems from natural and synthetic polymers. Materials science monographs. Elsevier, Amsterdam
2. Salmén L (1990) In: Passaretti JD, Caulfield D, Roy R, Setterholm V (eds.) Materials interactions relevant to the pulp, paper, and wood industries. Material research society symposium proceedings, Pittsburgh, USA
3. Salmén NL (1982) Temperature and water induced softening behaviour of wood fibre based materials, PhD thesis, Royal Institute of Technology, KTH, Stockholm
4. Rautkari L, Laine K, Laflin N, Hughes M (2011) J Mater Sci 46:4780. doi:10.1007/s10853-011-5458-z
5. Rautkari L, Laine K, Kutnar A, Medved S, Hughes M (2013) J Mater Sci 48:2370. doi:10.1007/s10853-012-7019-5
6. Rautkari L (2012) Surface modification of solid wood using different techniques. Doctoral dissertation. Aalto University, Department of Forest Products Technology, Espoo, Finland
7. Laine K, Rautkari L, Hughes M, Kutnar A (2013) Eur J Wood Prod 1:17
8. Kutnar A, Laine K, Rautkari L, Hughes M (2012) Eur J Wood Prod 70:727
9. Jia D, Afzal MT, Gong M, Bedane AH (2010) IJE 4:191
10. Thoemen H, Humprey PE (2003) Wood Fiber Sci 35:456
11. Thoemen H, Humphrey PE (2006) Holz Roh Werkst 64:1
12. Dai C, Yu C (2004) Wood Fiber Sci 36:585
13. Zhou C, Dai C, Smith GD (2011) Compos B 42:1357
14. Kavazovic Z, Cloutier A, Fortin A, Deteix J (2008) Sensitivity study of a numerical model of heat and mass transfer involved during MDF hot PRESSING Process. In: Proceedings of the 51th international convention of society of wood science and technology, Conception, Chile
15. Di Blasi C (1998) Chem Eng Sci 53:353
16. Stanish MA, Schajer GS, Ferhan Kayıhan F (1986) AIChE J 32:1301
17. Younsi R, Kocaefe D, Poncsak S, Kocaefe Y (2006) AIChE J 52:2340
18. Kocaefe D, Younsi R, Poncsak S, Kocaefe Y (2007) Int J Therm Sci 46:707
19. Younsi R, Kokaefe D, Poncsak S, Junjun T (2008) Int J Model Simul 28:117
20. Perré P, Turner IW (1999) Int J Heat Mass Transf 42:4501
21. Perré P (2011) On the importance of the temperature level on coupled heat and mass transfer in wood and lignocellulosic biomass: fundamental aspects, formulation and modeling. In: Proceedings of the 3rd European Drying Conference, Palma, Spain
22. Perré P (2010) Dry Technol 28:944
23. Abaqus/Standard. Theory Manual. Version 6.8. (2008) Dassault Systèms Simulia Corp. Providence
24. Abaqus/Standard. User Manual. Version 6.8. (2008) Dassault Systèms Simulia Corp. Providence
25. Fortino S, Mirianon F, Toratti T (2009) Mech Time Dep Mater 13:333
26. Frandsen HL (2005) Modelling of moisture transport in wood—State of the art and analytic discussion. Wood science and timber engineering, Paper no. 1, 2nd ed., ISSN: 1395-7053 R0502, Department of Building Technology and Structural Engineering, Aalborg University
27. Stamm AJ (1964) Wood and cellulose science. The Ronald Press Company, New York
28. Frandsen HL (2007) Selected Constitutive models for simulating the hygromechanical response of wood. Dissertation no. 10. Department of Civil Engineering, Aalborg University, ISSN: 1901-7294
29. Engelund ET, Thygesen LG, Svensson S, Hill CAS (2013) Wood Sci Technol 47:141
30. Siau JF (1984) Transport processes in wood. Springer, Berlin
31. Eckelman CA, Baker JL (1976) Heat and air requirements in the Kiln drying of wood. Research Bulletin no. 933. Department of Forestry and Natural Resources and Agricultural Engineering, Purdue University
32. Hozjan T, Svensson S (2011) Holzforschung 65:97
33. Mackenzie-Helnwein P, Hanhijärvi A (2003) J Eng Mech 129:1006
34. Nairn JA (2006) Wood Fiber Sci 38:576
35. Oudjene M, Khelifa M (2009) Const Build Mater 23:3359